

The Replacement of $[\text{HgO}_2]^{2-}$ by the Tetrahedral Sulfate Anion $[\text{SO}_4]^{2-}$ in the Hg-1201 Superconductor

S. M. Loureiro,* P. G. Radaelli,† E. V. Antipov,*‡ J. J. Capponi,* B. Souletie,§
M. Brunner,§ and M. Marezio,*¶

*Laboratoire de Cristallographie, CNRS-UJF, BP 166, 38042 Grenoble Cedex 09, France; †ILL, BP 156, 38042 Grenoble Cedex 09, France; ‡Department of Chemistry, Moscow State University, 119899 Moscow, Russia; §CRTBT, CNRS-UJF, BP 166, 38042 Grenoble Cedex 09, France; and ¶AT&T, Bell Laboratories, Murray Hill, New Jersey 07974

Received September 29, 1995; accepted October 9, 1995

DEDICATED TO THE MEMORY OF ALEXANDER F. WELLS

The possibility of existence of a $\text{Hg}_{1-x}\text{S}_x\text{Ba}_2\text{CuO}_{4+2x+\delta}$ solid solution [(Hg, S)-1201] was studied at 18 kbar and 920°C. Monophasic samples were obtained in the range $0.00 \leq x \leq 0.15$, where the unit cell parameters were found to vary from $a = 3.8685(1)$ Å, $c = 9.4667(2)$ Å for $x = 0.00$ to $a = 3.9010(1)$ Å and $c = 9.3048(6)$ Å for $x = 0.15$. Samples with $x \geq 0.20$ were polyphasic and the unit cell parameters of the [(Hg, S)-1201] phases were found to vary up to $a = 3.9072(1)$ Å, $c = 9.2654(5)$ Å for a nominal composition $x = 0.30$. The as-prepared phases with $0.00 \leq x \leq 0.05$ were found to be nonsuperconducting due to overdoping, while superconductivity appeared at $x = 0.10$ ($T_{c,\text{onset}} = 40$ K). T_c increases with the amount of sulfate substitution due to the decrease of the average copper valence. For the annealed samples, the variation is opposite to that found for the as-prepared samples, $T_{c,\text{onset}}$ being higher for the sulfur-free phase. Rietveld refinements of neutron powder diffraction data has determined $\approx 18\%$ of the HgO_2^{2-} dumbbells to be substituted by SO_4^{2-} groups. In this structure the SO_4^{2-} anion adopts an average S–O bond length that is slightly higher than those in BaSO_4 . © 1996 Academic Press, Inc.

INTRODUCTION

$\text{HgBa}_2\text{CuO}_{4+\delta}$ was the first member of the $\text{HgBa}_2\text{Ca}_{n-1}\text{Cu}_n\text{O}_{2n+2+\delta}$ homologous series to be synthesized by Putilin *et al.* (1). Its relatively high T_c for one CuO_2 superconductor (94 K) generated a great interest for the properties of this phase and related compounds. Studies regarding the synthesis techniques and the variations of the extra oxygen content both in the overdoped (2, 3) and underdoped (4, 5) regions have also been extensively carried out. A variety of studies have been dedicated to cation substitutions such as with Pb and Bi, the lanthanides Pr and Ce, or the *d* transition elements Ti, V, Cr, Mo, or W (6–14). However, all these substitutions resulted in a decrease of the super-

conducting transition temperature for the corresponding phases.

On the other hand it has been shown that layered Cu-mixed oxides containing layers of oxyanions sandwiched between two SrO or (Ba, Sr)O layers (15, 16) can be synthesized. In the structures of the $\text{HgBa}_2\text{Ca}_{n-1}\text{Cu}_n\text{O}_{2n+2+\delta}$ homologous series it is possible to replace $[\text{HgO}_2^{2-}]$ with oxyanions as these are located between two BaO layers. The incorporation of carbonate groups in the Hg cuprates and its effect on the superconducting properties has already been investigated for the third and fourth members of the series by Kopnin *et al.* (17). However, carbonate- and nitrate-containing Cu mixed oxides have limitations regarding their thermal stability (18). Tetrahedral oxyanions such as sulfates or phosphates have also been successfully incorporated into the structures of layered Cu-mixed oxides such as $(\text{Y, Sr, Ca})\text{Sr}_2\text{Cu}_{2.8}(\text{MO}_4)_{0.2}\text{O}_{6.2}$ [$M = \text{S, P}$], where $\approx 25\%$ of the Cu cations of the reservoir blocks were substituted by SO_4^{2-} or PO_4^{3-} anions (18). Our aim in the present work was to study the possibility of replacing in the Hg-1201 phase $[\text{HgO}_2^{2-}]$ by tetrahedral sulfate oxyanions, and to study its effect on the structural and superconducting properties.

EXPERIMENTAL

A precursor with the nominal composition Ba_2CuO_y was prepared by mixing high-purity oxides (BaO_2 [Aldrich, 95%] and CuO [Aldrich, 99%]) in an agate mortar. The mixture was placed in a tubular furnace at 830°C under an oxygen flow for 10 h, following the procedure described in Ref. (3). This precursor was then mixed in a glove box with the amounts of HgO [Aldrich, 99%], BaSO_4 [Rec-tapur, >98%] and CuO , [Aldrich, 99%] necessary to prepare phases with sequential stoichiometries $0.00 \leq x \leq$

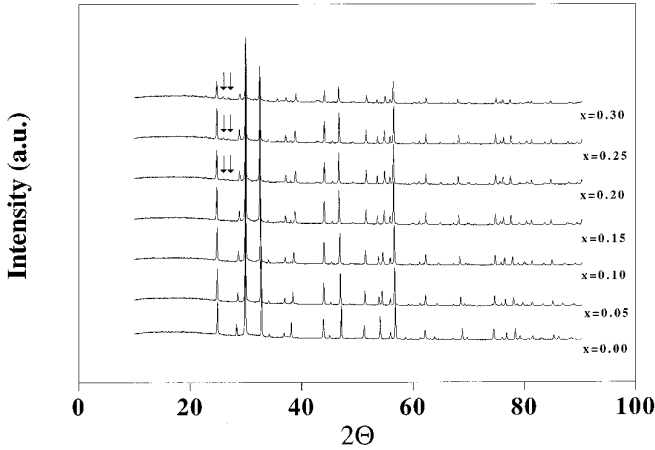


FIG. 1. X-ray powder patterns of the $\text{Hg}_{1-x}\text{S}_x\text{Ba}_2\text{CuO}_{4+2x+\delta}$ phases, with $0.00 \leq x \leq 0.30$ [$\Delta x = 0.05$].

0.30 [$\Delta x = 0.05$], $x = 0.50, 0.75$, and 1.00 of the general formula $\text{Hg}_{1-x}\text{S}_x\text{Ba}_2\text{CuO}_{4+2x+\delta}$. Gold capsules containing the samples were placed in a cell appropriate for high-pressure high-temperature synthesis. These cells were then placed in a belt-type apparatus and the pressure was raised up to 18 kbar, after which the temperature was increased up to 920°C and kept fixed for 0.6 h. Subsequently the current was turned off and the pressure decreased to the ambient value. The capsules were open and the products were placed immediately in a glove box filled with dry argon. The annealing treatments were performed in a tubular furnace under a flow of pure argon at 250°C for 10 h.

X-ray powder data were collected between 10° and 90°, using a Siemens D5000 powder diffractometer in transmission mode, equipped with a Ge monochromator placed on the primary beam ($\text{CuK}\alpha_1$ radiation, $\lambda = 1.54056 \text{ \AA}$), a rotating sample holder and a mini PSD.

A.C. susceptibility measurements were made using an a.c. susceptometer with a field of 0.4 Oe at 119 Hz. In order to get a correct evaluation of the superconducting volumes, the measurements were performed on finely ground powder samples. The temperature was measured with calibrated Pt and Ge 100 Ω thermometers.

X-RAY POWDER AND a.c. SUSCEPTIBILITY CHARACTERIZATION

The X-Ray powder patterns of the samples with $0.00 \leq x \leq 0.30$ are shown in Fig. 1. The samples with nominal composition $0.00 \leq x \leq 0.15$ were found to be monophasic. For $x = 0.20$, however, small quantities of BaSO_4 (marked by an arrow) as well as CuO appeared and their content increased with increasing x . The X-ray powder pattern of the sample with $x = 0.00$ was indexed on the $P4/mmm$ space group with unit cell parameters $a = 3.8685(1) \text{ \AA}$,

$c = 9.4667(2) \text{ \AA}$. These are typical values for an overdoped Hg-1201 phase (2, 3). The phase with $x = 0.05$ showed a significant increase of the a -parameter to $a = 3.8819(1) \text{ \AA}$ as well as a significant decrease of the c -parameter to $c = 9.3949(2) \text{ \AA}$. Up to $x = 0.15$, the unit cell parameters follow this general trend, this concentration representing the limit between mono and polyphasic regions (see Fig. 2). It has to be pointed out that the simultaneous increase and decrease of the a - and c -parameters, respectively, cannot be obtained by extra oxygen doping alone (2). Therefore, the variation of the unit cell parameters is a confirmation that sulfate has in fact entered the structure. However, for the polyphasic samples with $0.20 \leq x \leq 0.50$ the well-defined increase and decrease are not observed any longer and one can only draw a dashed guide line parallel to the abscissa (see Fig. 2). In this region, however, the unit cell parameters are not constant as a function of the nominal composition, probably due to an imperfect control of the thermodynamic parameters during the high-pressure synthesis. For some samples, like the $x = 0.25$, the rather large value of the c -parameter and the small value of the a -parameter seem to indicate that the real composition lies in the $0.15 \leq x \leq 0.20$ range. On the other hand, the unit cell parameters of the 1201 phase obtained in the polyphasic $x = 0.30$ sample ($a = 3.9072(1) \text{ \AA}$, $c = 9.2654(5) \text{ \AA}$) are consistent with a real composition somewhat greater than 0.20. This observation leads us to conclude that the real limit for the solid solution is slightly higher than the 15% obtained for the monophasic sample.

The samples with nominal composition $x = 0.50, 0.75$, and 1.00 were also prepared under the same experimental conditions but with a different precursor. The sulfate-substituted Hg-1201 phase was identified in the samples with $x = 0.50$ and 0.75 but with a much smaller fraction and

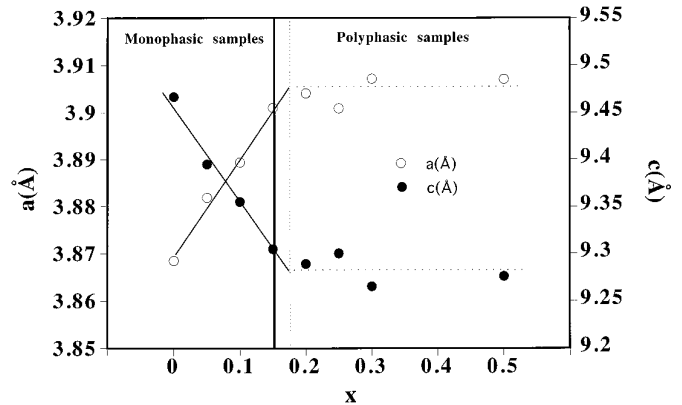


FIG. 2. Unit cell parameters a (white circles) and c (black circles) vs x for the as-prepared $\text{Hg}_{1-x}\text{S}_x\text{Ba}_2\text{CuO}_{4+2x+\delta}$ samples with $0.00 \leq x \leq 0.30$ [$\Delta x = 0.05$] and 0.50. Error bars are smaller than the symbols. Lines through the points are guides for the eye. The vertical dotted line indicates the limit between monophasic (left) and polyphasic (right) samples.

TABLE 1

Unit Cell Parameters and $T_{c,onset}$ Values as a Function of x ($x =$ Nominal Sulfate Content) for the $\text{Hg}_{1-x}\text{S}_x\text{Ba}_2\text{CuO}_{4+2x+\delta}$ Phases with $0.00 \leq x \leq 0.30$ [$\Delta x = 0.05$] and $x = 0.50$

x	a (Å)	c (Å)	$T_{c,onset}$ (K)
0.00	3.8685(1)	9.4667(2)	0
0.05	3.8819(1)	9.3949(2)	0
0.10	3.8894(1)	9.3550(5)	41
0.15	3.9010(1)	9.3048(6)	62
0.20	3.9041(1)	9.2890(5)	65
0.25	3.9009(1)	9.3003(4)	63
0.30	3.9072(1)	9.2654(5)	73
0.50	3.9071(3)	9.276(3)	71

these samples contained large amounts of impurities such as BaSO_4 and CuO . The sample with $x = 1.00$, in addition to the impurities found with $x = 0.50$ and 0.75 , contained also BaCuO_2 as well as other unidentified phases, but no trace of the 1201 phase was detected. The a -unit cell parameter of the sulfate-substituted Hg-1201 phase obtained in the sample with nominal composition $x = 0.50$ was found to be (within the error bars) the same as the a -parameter of that with $x = 0.30$ [$a = 3.9071(3)$ Å], but the c -parameter was slightly larger [$c = 9.276(3)$ Å], being more consistent with a composition in the interval $0.20 \leq x \leq 0.30$. The values of the unit cell parameters as a function of the nominal composition x are plotted in Fig. 2 and reported in Table 1.

The sulfate incorporation can be monitored by the variation of the intensities of some reflections that are strongly affected by this substitution. The Lazy program [1991–92, V2] was used to calculate the theoretical diffraction patterns of different $\text{Hg}_{1-x}\text{S}_x\text{Ba}_2\text{CuO}_{4+2x+\delta}$ phases [$0.00 \leq x \leq 0.20$], and the intensities of all the major reflections were followed in order to observe which were the most affected by the substitution. Only the decrease of the scattering factor of the Hg-site was taken into consideration. The relative intensities [I_{hkl}/I_{102}] of the 101 and 103 reflections follow opposite variations. The 101 reflection shows the most significant decrease while the 103 reflection shows a considerable increase with increasing x . These reflections were followed in the experimental X-ray powder patterns. The results are given in Table 2. It can be seen, as expected, that the relative intensity of the 101 reflections *decreases* and that of the 103 reflection *increases* with increasing x . In agreement with the variation of the unit cell parameters, the relative change of the 101/103 intensities supports the conclusion that sulfate groups are gradually incorporated into the structure.

The values of $T_{c,onset}$ for the as-prepared samples with $0.00 \leq x \leq 0.50$, as obtained from a.c. susceptibility measurements, are reported in Table 1. The a.c. susceptibility

TABLE 2

Observed Relative Intensities of the 101 and 103 Reflections of the $\text{Hg}_{1-x}\text{S}_x\text{Ba}_2\text{CuO}_{4+2x+\delta}$ Phases with $0.00 \leq x \leq 0.20$

x	I_{101}	I_{103}
0.00	0.301	0.040
0.05	0.279	0.042
0.10	0.262	0.054
0.15	0.251	0.060
0.20	0.252	0.065

vs temperature curves for the as-prepared samples with $0.10 \leq x \leq 0.50$ are shown in Fig. 3. The samples with $x = 0.00$ and 0.05 were found to be nonsuperconducting. As stated above, this result is consistent with the already published results for highly overdoped nonsuperconducting Hg-1201 phases (2, 3). Superconductivity appears for $x = 0.10$. The $T_{c,onset}$ is 41 K but the transition is quite broad. The sample with $x = 0.15$ exhibits a sharp transition with an onset at 62 K. The $T_{c,onset}$ increases slightly to 65 K for $x = 0.20$, but decreases to 63 K for $x = 0.25$. The a.c. susceptibility measurements seem to corroborate our supposition that the real stoichiometry of the [(Hg, S)-1201] phase obtained in the sample with nominal composition $x = 0.25$ would in fact lie between $x = 0.15$ and $x = 0.20$. The sample with nominal composition $x = 0.30$ exhibits a sharp transition with a $T_{c,onset}$ at 73 K. This phase is then the most reduced within the isolated products. The sample with $x = 0.50$ had a much smaller superconducting volume and a $T_{c,onset}$ at 71 K. The data are in agreement with both the small phase fraction and the unit cell parameters found by X-ray powder diffraction, as discussed above.

The unit cell parameters and the superconducting critical

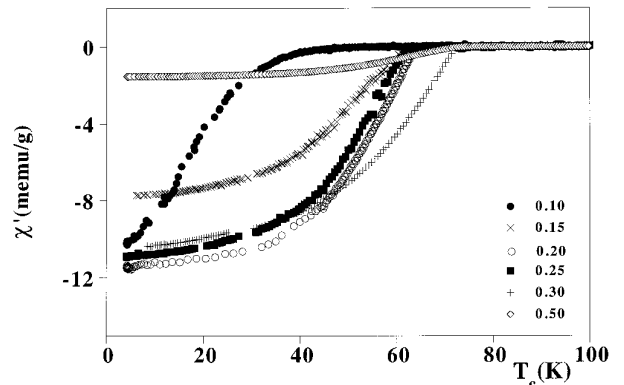


FIG. 3. a.c. susceptibility vs temperature for the as-prepared $\text{Hg}_{1-x}\text{S}_x\text{Ba}_2\text{CuO}_{4+2x+\delta}$ samples, with $0.00 \leq x \leq 0.30$ [$\Delta x = 0.05$] and $x = 0.50$.

TABLE 3

Unit Cell Parameters and $T_{c,onset}$ for the $x = 0.00$ and 0.15 $Hg_{1-x}S_xBa_2CuO_{4+2x+\delta}$ Phases Annealed at 250°C for 10 h Argon Flow

x	a (Å)	c (Å)	$T_{c,onset}$ (K)	$ \Delta a $	$ \Delta c $
0.00	3.8803(1)	9.504(1)	88	0.0118	0.037
0.15	3.9060(1)	9.304(1)	77	0.005	0.001

temperatures for the $x = 0.00$ and 0.15 samples after argon annealing are reported in Table 3. A.C. susceptibility vs temperature curves are shown in Fig. 4. In both cases, unit cell parameter a increases upon annealing, which is consistent with a reduction of the copper oxidation state. The simultaneous increase of T_c confirms that the as-prepared samples are overdoped.

NEUTRON POWDER DIFFRACTION

Time-of-flight neutron powder diffraction data were obtained on the as-prepared sample with nominal composition $x = 0.15$ at room temperature using the POLARIS diffractometer at the ISIS facility of the Rutherford Appleton Laboratory. The sample, weighing ≈ 0.2 g, was contained in a vanadium can during the measurement. Only the backscattering data ($2\theta = 145^\circ$) were employed in the refinements. Before the refinements, raw data were normalized to the incident spectrum and corrected for absorption based on the geometrical shape and the apparent density of the powder, the statistical errors being propagated through the correction process. Structural parameters were refined by the Rietveld method, using the GSAS program by Larsen and Von Dreele (20). Bragg peaks from the vanadium can and a small amount of BaSO₄ were fitted as additional phases during the refinement.

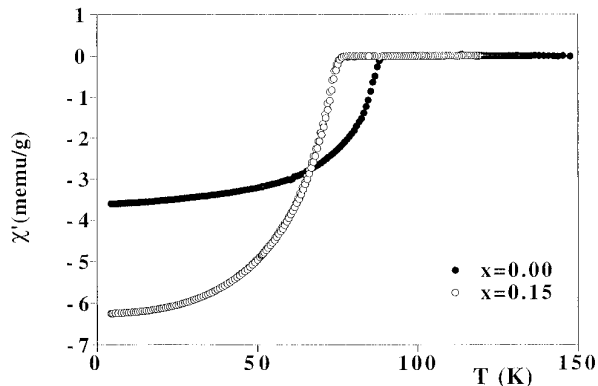


FIG. 4. a.c. susceptibility vs temperature for the annealed $Hg_{1-x}S_xBa_2CuO_{4+2x+\delta}$ samples, with $x = 0.00$ and $x = 0.15$.

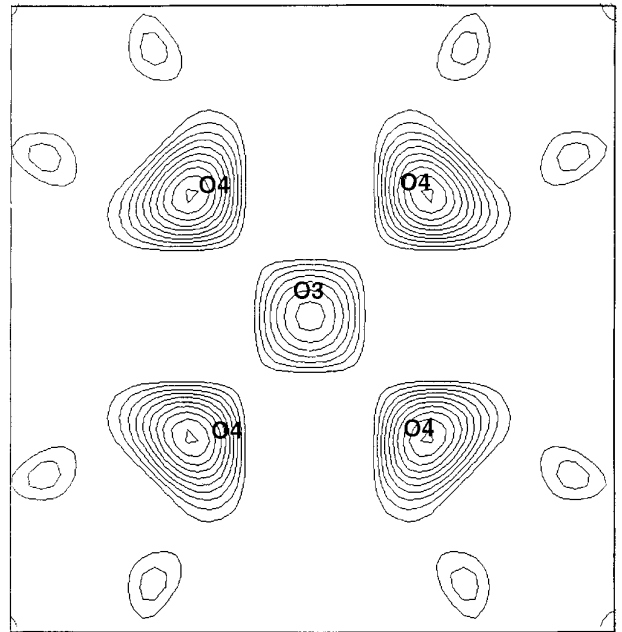


FIG. 5. Section of a difference fourier map showing a portion of the $[x, y, 0]$ plane of the $Hg_{1-x}S_xBa_2CuO_{4+2x+\delta}$ ($x = 0.15$) structure. Observed and calculated intensities were obtained using the “ideal” Hg-1201 without additional oxygen (see text). The map size (center to edge) is 1.4 \AA . Contours are drawn every $0.02 \times 10^{-12} \text{ cm}^3/\text{\AA}^3$, starting from $0.04 \times 10^{-12} \text{ cm}^3/\text{\AA}^3$. The labels indicate the appropriate positions of the O3 and O4 atoms used in subsequent refinements (see text).

An initial set of refinement cycles were performed based on the “ideal” 1201 structure. Attempts to refine the occupancy factors resulted in reduced values for mercury and the apical oxygen O2 (70–80% of full occupancy). This model was then employed to extract “observed” integrated intensities, which allowed difference Fourier maps (DFM) to be constructed. After a peak search, followed by visual inspection of the maps, the following observations were made:

(1) The strongest peaks in the DFM are located on the mercury plane. Besides a strong peak centered on $[1/2, 1/2, 0]$, corresponding to the usual location of additional oxygen in Hg-1201, four “satellite” peaks are also present, with approximate coordinates $[\pm 1/3, \pm 1/3, 0]$. A DFM section of the $[x, y, 0]$ plane is shown in Fig. 5.

(2) Strong peaks in the DFM were also located between the Hg and O2 positions, with approximate coordinates $[0, 0, 0.14]$. These maxima are rather extended in the plane perpendicular to the z -axis.

It is noteworthy that the additional maxima can be arranged in a somewhat distorted tetrahedron, with vertices at $[0, 0, \pm 0.14]$ and $[\pm 1/3, 1/3, 0]$ or at symmetry-equivalent positions. Furthermore, the distance between the vertices and the center of this tetrahedron is of the order of 1.5 \AA ,

TABLE 4
Structural Parameters of $\text{Hg}_{1-x}\text{S}_x\text{Ba}_2\text{CuO}_{4+2x+\delta}$, as Obtained from Rietveld Refinements of Time-of-Flight Neutron Powder Diffraction Data

Atom	x	y	z	B (\AA^2)	Mult.	Fract. Occ.
Hg	0	0	0	0.89(7)	1	0.743(14)
Ba	0	0	0.29267(24)	0.71(5)	2	1.0000
Cu	0	0	0.5	0.44(5)	1	1.0000
O1	0	0	0.5	0.53(5)	2	1.0000
O2	0	0	0.2153(4)	1.0(1)	2	0.800(17)
O3	0.5	0.5	0	1.0	1	0.150(14)
S	0	0.139(4)	0	1.0	4	0.046(3) ^a
O4	0.3297(33)	0.372(5)	0	1.0	8	0.046(3) ^a
O5	0	-0.095(5)	0.1383(14)	1.0	8	0.046(3) ^a

Note. The space group is $P4/mmm$. The unit cell parameters and cell volume are $a = b = 3.8986(2)$, $c = 9.2466(6)$ \AA ; $V = 141.30(1)$ \AA^3 . Phase fractions: Vanadium, 83.25%; $\text{Hg}_{1-x}\text{S}_x\text{Ba}_2\text{CuO}_{4+2x+\delta}$, 16.5%; BaSO_4 , 0.258%. The number in parenthesis are statistical errors of the last significant digits (when absent, the parameter was held fixed). The site symmetry and the fractional occupancy of each site are reported in the last two columns. The number of atoms/f.u. can be obtained multiplying the site symmetry by the fractional occupancy. $R_{\text{wp}} = 1.26\%$; $R(F^2) = 10.2\%$; $\chi^2 = 2.54$.

^a Constrained to be equal.

hence comparable with typical S–O distances in sulfates (21). It is therefore reasonable to hypothesize that these maxima correspond to oxygen atoms belonging to sulfate groups SO_4^{2-} , which, in this case, would replace HgO_2^- dumbbells. On the basis of this hypothesis, subsequent refinement cycles were performed introducing three additional oxygen sites: O3 at $[1/2, 1/2, 0]$ (the “normal” position for interstitial oxygen in Hg-1201); O4 at $[x, x, 0]$, $x \sim 1/3$ and O5 at $[0, 0, z]$, $z \sim 0.14$. Positions and occupancies can be refined independently for all these atoms, although it is necessary to make reasonable assumptions about their thermal parameters. In particular, the refined occupancies of the O3, O4, and O5 sites would correspond

to approximately 0.125(12), 0.26(2), and 0.24(2) atoms/f.u., respectively.

At this stage, however, two difficulties arose: first, sulfur cannot be satisfactorily introduced in the refinements. In fact, the center of gravity of the aforementioned O_4 tetrahedron would be located at $[x, 0, 0]$ with $x \sim 0.15$. This site is too close to the Hg site to be refined independently, given the fact that such an amount of sulfur would correspond to less than 3% of the mercury setting. Second, setting O4 and O5 on the $[x, x, 0]$ and $[0, 0, z]$ special positions constrains the dihedral angle perpendicular to the z -axis to be 90° (it is 70.32° in a regular tetrahedron). Although it is quite likely that the SO_4 tetrahedron is indeed somewhat distorted (as it is, for instance, in BaSO_4 (21), there is no *a priori* reason to assume such a large distortion. On the other hand, some assumptions have to be made to assure the stability of the refinement. A reasonable compromise is to impose a so-called rigid body constraint. In this scheme, S, O4, and O5 are constrained to lay at the center and on the vertices of a regular tetrahedron, respectively. The single S–O distance (constrained to be equal for O4 and O5), as well as the position of the tetrahedron in the cell can be refined. For simplicity, the sulfur atom was placed on a $[0, y, 0]$ site and the three occupancy factors $f(\text{O4})$, $f(\text{O5})$, and $f(\text{S})$ were constrained to be equal. Due to the different site multiplicity, this constraint imposes the correct ratios between sulfur and oxygen in the SO_4 groups. The refined values of $f(\text{O4})$, $f(\text{O5})$, and $f(\text{S})$ are consistent with a sulfate content of 0.18(1) mols/f.u. The refined structural parameters using this model are reported in Table 4. Selected bond distances are reported in Table 5. A Rietveld plot and a schematic drawing of the structure are shown in Figs. 6 and 7, respectively.

TABLE 5
Selected Bond Distances for $\text{Hg}_{1-x}\text{S}_x\text{Ba}_2\text{CuO}_{4+2x+\delta}$, as Obtained from Rietveld Refinements of Time-of-flight Neutron Powder Diffraction Data

Bond pair	Bond length (\AA)
Hg–O2	2.001(4)
Hg–O3	2.75672(13)
Ba–O1	2.7413(16)
Ba–O2	2.8491(11)
Ba–O3	2.7209(22)
Cu–O1	1.94930(9)
Cu–O2	2.647(4)
S–O4	1.574(16) ^a
S–O5	1.574(16) ^a

^a Constrained to be equal.

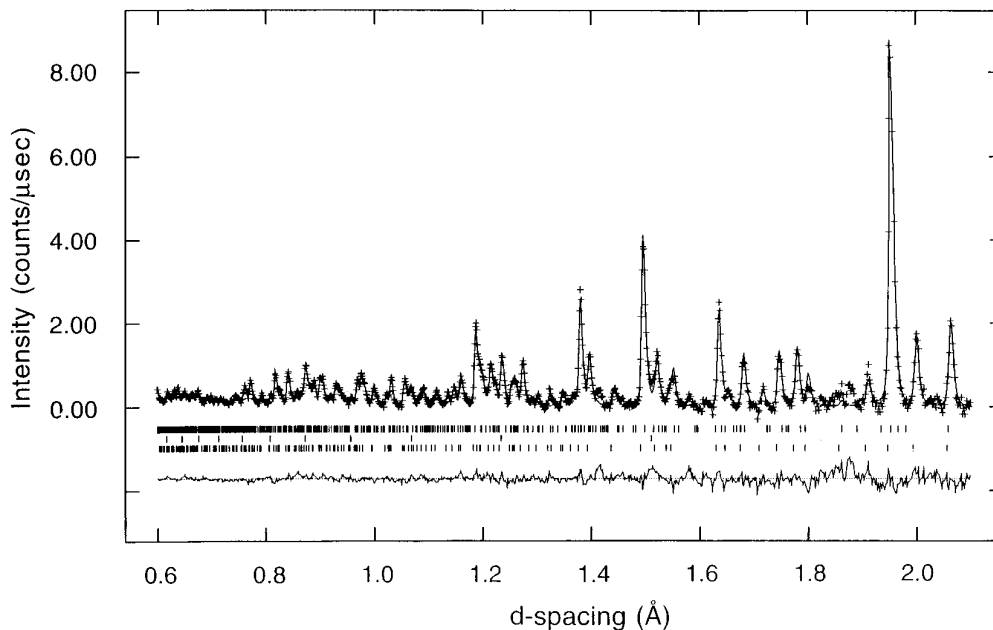


FIG. 6. Rietveld refinement profile for the $\text{Hg}_{1-x}\text{S}_x\text{Ba}_2\text{CuO}_{4+2x+\delta}$ ($x = 0.15$) sample. The plus (+) signs are the time-of-flight neutron powder diffraction data, after normalization with respect of the incident spectrum and adsorption correction. The solid line is the calculated profile. Tick marks below the diffraction profile indicate the position of the Bragg reflections for Hg-1201, vanadium, and BaSO_4 , from bottom to top. The background was fitted as part of the refinement, but was subtracted before plotting. A difference curve (observed minus calculated) is plotted at the bottom.

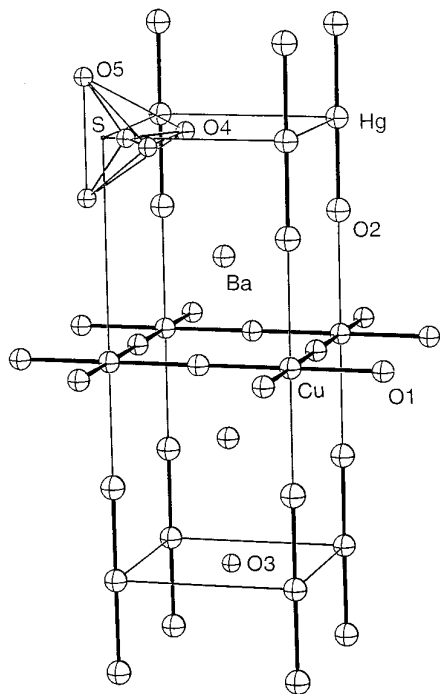


FIG. 7. Structure of $\text{Hg}_{1-x}\text{S}_x\text{Ba}_2\text{CuO}_{4+2x+\delta}$, as determined from the present work. The c -axis is in the vertical direction. An SO_4 group is shown in the top left corner of the unit cell, with the bonding emphasizing the tetrahedral coordination. Thermal ellipsoids are drawn at 70% probability.

Analysis of the time-of-flight neutron powder diffraction data, therefore, confirms the substitution of approximately 18% of the HgO_2^{2-} dumbbells with SO_4^{2-} groups. Since the two groups have the same electrical charge, this substitution does not contribute to the overall doping of the compound. However, a substantial amount of additional oxygen was found in the “interstitial” position $[1/2, 1/2, 0]$, indicating that the compound is strongly overdoped. This is consistent with the thermal annealing result on the as-prepared $x = 0.15$ sample. This process increased the T_c of the treated sample while simultaneously increasing the a -parameter, which indicates that some oxygen in the $(1/2, 1/2, 0)$ position has been removed and the copper valence has been reduced. Rietveld refinements employing the Rigid Body Constraint indicate that sulfur is displaced up to 0.5 \AA from the $[0, 0, 0]$ position, and is at the center of an O_4 tetrahedron, with S–O distances of $1.57(2) \text{ \AA}$. This distance is longer by a few standard deviations than typical S–O distances in other sulfates (for example, in BaSO_4 , these distances vary between 1.48 \AA and 1.52 \AA). Although this result has to be taken rather cautiously, due to the simplified nature of the model employed in the refinements, such an elongation would not be impossible in the framework of the constraints imposed by the 1201 structure. The “displaced apical oxygen” O5 and the “displaced interstitial oxygen” O4, forming the O_4 tetrahedron, are both shifted by about 0.8 \AA with respect to the “ideal” sites O2 and O3. The reduction in occupancy of the O2

site is consistent, within the error bars, with the presence of 18% of O5, while the occupancy of the Hg site, even considering the SO₄ substitution, is a few standard deviations too low. It has to be pointed out, however, that previous refinements of the Hg-1201 structure based on powder neutron diffraction data have systematically yielded either a low occupancy or a large thermal parameter for the Hg site (22, 23). Although several models have been proposed, it is likely that this effect may arise, at least in our case, from a too simplistic model of the mercury static and/or dynamic displacements. This is also confirmed by the fact that Rietveld refinements of our X-ray powder diffraction data (not presented in this paper) yield a Hg occupancy of 0.822(3).

DISCUSSION

On the basis of the structural determination, the correlation between sulfate content and T_c for the as-prepared samples can be discussed in greater detail. As we have seen, neutron diffraction data indicate that SO₄²⁻ oxyanions replace HgO₂⁻ dumbbells. Therefore, this substitution does not contribute to the overall electrical doping of the compound. In Hg_{1-x}S_xBa₂CuO_{4+2x+δ}, doping is provided entirely by additional oxygen atoms O3 as it is in HgBa₂CuO_{4+δ}. Nonetheless, the increase of T_c as a function of the nominal sulfate content x is consistent with a reduction of the copper oxidation state, given the fact that all samples are in the overdoped region of the phase diagram. We shall therefore conclude that, at least for the as-prepared samples, the concentration δ of the “doping” O3 oxygen atoms *decreases* as x increases. The sign of the change in the a -axis as a function of x would also be consistent with a reduction of the copper valence. It has to be remarked, however, that the magnitude of this effect is too large to be solely due to extra oxygen doping and, has to come, at least in part, from the unit cell strain induced by the SO₄ incorporation. The reduction of the c -axis is consistent with the much shorter S–O distance as compared to the Hg–O bond length.

A simple explanation of the decrease of δ as a function of x is related to the average oxidation state of copper in the reactants. In fact, up to $x = 0.30$, all the samples were prepared with the same precursor Ba₂CuO_y, which consists of a mixture of phases where the average copper valence is greater than +2 (2). When BaSO₄ is added to introduce the sulfate oxyanion, the copper content of the reactant mixture has to be adjusted with CuO, where copper has a valence of exactly +2. As a consequence, the average copper valence in the precursor *decreases* as a function of sulfate content. This would be an explanation for the reduced valence of copper in the product *only* assuming that there is no loss of oxygen during the synthesis.

An alternative and perhaps better explanation can be

found based on the structural chemistry of the compound. As we have seen, neutron diffraction data analysis indicates that two of the oxygen atoms belonging to the SO₄ tetrahedra are located in the Hg plane. Consequently, as sulfate groups are introduced in the structure, less sites are available for the “doping” oxygen O3. The increase in interaction energy between oxygen atoms in the Hg plane would therefore justify a reduction of the O3 occupancy (and an increase of T_c) as a function of sulfate content at a given P_{O_2} .

It is very difficult to determine which of these explanations is correct. In fact, high-pressure synthesis takes place neither at constant oxygen stoichiometry nor at constant P_{O_2} , but rather in extreme nonequilibrium conditions.

Given the complex interplay between sulfur and oxygen doping in this compound, the direct effect of the sulfate substitution upon superconductivity cannot be conclusively determined from the present work. After annealing in argon under the same conditions, T_c for the sulfur-free sample is indeed higher than for the sulfate-containing one, but there is no evidence that these annealing conditions are optimal for the latter sample.

CONCLUSION

A solid solution with the tetrahedral sulfate oxyanion was found for the first member of the mercury-based superconducting mixed oxide series. This solid solution of composition Hg_{1-x}S_xBa₂CuO_{4+2x+δ} has a limit that lies between 15 and 20% of sulfate substitution. This substitution affects particularly certain reflections such as 101 and 103, which allowed us to follow the sulfate incorporation by determining the variation of the relative intensities. Neutron diffraction data analysis indicates that SO₄ tetrahedra replace HgO₂ dumbbells in the structure, and suggest that the S–O bond length might be slightly elongated with respect to the value found for BaSO₄. The refined occupancy of the doping oxygen O3 site is consistent with the sample examined being in the overdoped state. The sulfate incorporation brings about a reduction of the copper valence with respect to sulfur-free samples prepared under the same conditions, which causes a raise on the $T_{c,onset}$ of the as-prepared samples up to 73 K for $x = 0.30$ sulfate nominal composition.

ACKNOWLEDGMENTS

The authors thank Ron Smith for helpful cooperation during the neutron diffraction data collection at ISIS. Neutron powder diffraction data collection at ISIS was supported by the European Economic Community (EEC), through its Human Capital and Mobility Program for Large Scale Facilities. S.M.L. acknowledges the JNICT/PRAXIS XXI Program for the BD 3328/94 contract. E.V.A., J.J.C., and M.M. thank INTAS for Grant 93-2483. E.V.A. thanks the International Science Foundation (M1G000) and the Russian Scientific Council on Superconductivity for the partial support of this study.

REFERENCES

1. S. N. Putilin, E. V. Antipov, O. Chmaissem, and M. Marezio, *Nature* **362**, 226 (1993).
2. S. M. Loureiro, E. T. Alexandre, E. V. Antipov, J. J. Capponi, S. de Brion, B. Souletie, J. L. Tholence, and M. Marezio, *Physica C* **243**, 1 (1994).
3. E. T. Alexandre, S. M. Loureiro, E. V. Antipov, P. Bordet, S. de Brion, J. J. Capponi, and M. Marezio, *Physica C* **245**, 207 (1995).
4. M. A. Subramanian, "ICMAS-93 Superconducting Materials, Paris-France, 1993," p. 167. IITT-International.
5. Q. Huang, J. W. Lynn, Q. Xiong, and C. W. Chu, *Phys. Rev. B*, **52**, 462 (1995).
6. R. S. Liu, D. S. Shy, S. F. Hu, and D. A. Jefferson, *Physica C* **216**, 237 (1993).
7. F. Goutenoire, P. Daniel, M. Hervieu, G. van Tendeloo, C. Michel, A. Maignan, and B. Raveau, *Physica C* **216**, 243 (1993).
8. M. A. Subramanian and M.-H. Whangbo, *J. Solid State Chem.* **109**, 410 (1994).
9. J. Shimoyama, S. Hakahura, K. Kitazawa, K. Yamafuji, and K. Kishio, *Physica C* **224**, 1 (1994).
10. A. Maignan, D. Pelloquin, M. Hervieu, C. Michel, and B. Raveau, *Physica C* **243**, 214 (1995).
11. A. Maignan, D. Pelloquin, S. Malo, C. Michel, M. Hervieu, and B. Raveau, *Physica C* **243**, 233 (1995).
12. C. Michel, M. Hervieu, A. Maignan, D. Pelloquin, V. Badri, and B. Raveau, *Physica C* **241**, 1 (1995).
13. W. L. Lechter, L. R. Toth, M. S. Osofsky, E. F. Skelton, A. R. Drews, C. C. Kim, B. Das, S. B. Qadri, A. W. Webb, and R. J. Soulen Jr., *Physica C* **242**, 221 (1995).
14. O. Chmaissem, T. Z. Deng, and Z. Z. Sheng, *Physica C* **242**, 17 (1995).
15. D. V. Fomichev, A. L. Kharlanov, E. V. Antipov, and L. M. Kovba, *Superconductivity* **3**, 127 (1990).
16. C. Greaves and P. R. Slater, *Physica C* **175**, 172 (1991).
17. E. M. Kopnin, E. V. Antipov, J. J. Capponi, P. Bordet, C. Chaillout, S. de Brion, M. Marezio, A. P. Bobylev, and G. V. Tendeloo, *Physica C* **243**, 222 (1994).
18. C. Greaves, M. Al-Mamouri, P. R. Slater, and P. P. Edwards, *Physica C* **235-240**, 158 (1994).
19. E. V. Antipov, S. N. Putilin, E. M. Kopnin, J. J. Capponi, C. Chaillout, S. M. Loureiro, M. Marezio, and A. Santoro, *Physica C* **235-240**, 21 (1994).
20. A. C. Larsen and R. B. von Dreele, University of California—Report **LA-UR-86-748**, Los Alamos National Laboratory, 1985.
21. R. W. James and W. A. Wood, *Proc. R. Soc. A* **109**, 598 (1925).
22. O. Chmaissem, Q. Huang, S. N. Putilin, M. Marezio and A. Santoro, *Physica C* **212**, 259 (1993).
23. J. L. Wagner, P. G. Radaelli, D. G. Hinks, J. D. Jorgensen, J. F. Mitchell, B. Dabrowski, G. S. Knapp, and M. A. Beno, *Physica C* **210**, 447 (1993).